Microelectronics Reliability xxx (2011) xxx–xxx

Contents lists available at SciVerse ScienceDirect

Microelectronics Reliability

journal homepage: www.elsevier.com/locate/microrel

Study of the breakdown failure mechanisms for power AlGaN/GaN HEMTs implemented using a *RF* compatible process

Gang Xie [a,b], Edward Xu [a], Bo Zhang [b], Wai Tung Ng [a,*]

[a] The Edward S. Rogers Sr. Electrical and Computer Engineering Department, University of Toronto, Toronto, Ontario, Canada
[b] State Key Laboratory of Electronic Thin Films and Integrated Devices, University of Electronic Science and Technology of China, Chengdu, China

ARTICLE INFO

Article history:
Received 7 May 2011
Received in revised form 14 November 2011
Accepted 21 November 2011
Available online xxxx

ABSTRACT

The breakdown failure mechanisms for a family of power AlGaN/GaN HEMTs were studied. These devices were fabricated using a commercially available MMIC/*RF* technology with a semi-insulating SiC substrate. After a 10 min thermal annealing at 425 K, the transistors were subjected to temperature dependent electrical characteristics measurement. Breakdown degradation with a negative temperature coefficient of −0.113 V/K for the devices without field plate was found. The breakdown voltage is also found to be a decreasing function of the gate length. Gate current increases simultaneously with the drain current during the drain-voltage stress test. This suggests that the probability of a direct leakage current path from gate to the 2-DEG region. The leakage current is attributed by a combination of native and generated traps/defects dominated gate tunneling, and hot electrons injected from the gate to channel. Devices with field plate show an improvement in breakdown voltage from ~40 V (with no field plate) to 138 V and with lower negative temperature coefficient. A temperature coefficient of −0.065 V/K was observed for devices with a field plate length of 1.6 μm.

1. Introduction

There has been extensive interest in wide bandgap semiconductors for high power electronic applications [1–3]. AlGaN/GaN HEMTs have received much attention for their ability to operate at high-power levels because of their high breakdown field, high electron mobility (more than 2000 $cm^2\ V^{-1}\ s^{-1}$) [4], and high temperature operation. Mizuno et al. pointed out that the main issue with the Schottky gate AlGaN/GaN HEMT is its relatively large gate leakage current [5]. Mishra et al. proposed a SiO_2/Si_3N_4 bi-layer structure as the gate insulator [6]. Even though these MIS-FET approaches are promising, it is still important to study HEMTs with a Schottky gate because most of the GaN devices under development are HEMTs.

Most work on HEMTs has been focused on understanding and improving the performance such as the breakdown voltage, *BV*, and the specific on-resistance, $R_{on\text{-}sp}$. Breakdown voltage is affected by many factors, including device geometry, surface engineering [7], substrate engineering [8], etc. Based on these previous publications, reliability issues need to be solved urgently before these devices can be put into real applications. Therefore it is important to detect and to understand the possible degradation mechanisms. However, the breakdown failure mechanism for *RF* process based power AlGaN/GaN HEMTs is still not well understood, especially when operating under elevated temperatures. Reliability of these devices under harsh environment such as high drain voltage and high temperature is needed in many demanding applications. The temperature dependent measurement is commonly used to investigate the breakdown failure mechanism [9]. Ohno et al. explained that the breakdown mechanism in high power devices was mainly due to the impact ionization in the channel [10]. While Kotani et al. pointed out that the main reason was attributed by the electron hopping in the surface [11]. These theories are contradictory and are not sufficient to understand the breakdown failure mechanism of power AlGaN/GaN HEMTs.

In this paper, we have studied the breakdown failure mechanism in detail by investigating the temperature dependency of the drain to source leakage and the drain to gate leakage. We have also conducted an experiment to determine the dependence of the gate leakage and breakdown voltage on the gate length. Breakdown failures induced by large gate leakage current is mainly due to trap/defect-assisted tunneling and by the hot carrier injection near the gate electrode.

2. Experiment

The power AlGaN/GaN HEMTs were fabricated using a 3-in. *RF* GaN-on-SiC process. The epitaxial layer structure consists of an unintentionally doped AlGaN barrier layer (20 nm)/i-AlN spacing layer (1 nm)/i-GaN channel layer (200 nm)/C-doped insulating layer (2 μm)/AlN nucleation layer (20 nm). Al mole fraction in the AlGaN

* Corresponding author. Tel.: +1 416 946 5086; fax: +1 416 971 2286.
E-mail addresses: xielyz@vrg.utoronto.ca (G. Xie), ngwt@vrg.utoronto.ca (W.T. Ng).

0026-2714/$ - see front matter © 2011 Elsevier Ltd. All rights reserved.
doi:10.1016/j.microrel.2011.11.022

layer was 0.28. Sheet carrier density of 1.1×10^{13} cm^{-2} and electron mobility of 1800 cm^2 V^{-1} s^{-1} were obtained by Hall measurements. The device was first isolated by mesa etching. This is followed by the formation of the Ohmic contact using e-beam evaporated Ti/Al/Ni/Au (285 nm) with an annealing at 850 °C for 30 s in N_2 ambient. The Schottky contact was also formed by e-beam evaporated, un-annealed Ni/Au (430 nm) using photolithography and lift-off processes. Au was used to prevent oxidation and to provide a current path with low sheet resistance. The first 50 nm Si_3N_4 passivation film was deposited followed by the first layer of 1000 nm Au metallization. A second Si_3N_4 passivation film of 100 nm thick was also deposited to serve as a dielectric layer for the *MIM* capacitors. Finally, a second layer of 1000 nm thick Au was deposited and lifted off. This serves as a metal plate for the capacitor as well as the air-bridge for the multi-finger device configuration. Gate length of 0.8 μm, 2 μm and 3 μm were fabricated with the gate width of 80 μm. The drain to gate (L_{gd}) length was 2.1 μm. The cross-sectional view of a typical device is as shown in Fig. 1.

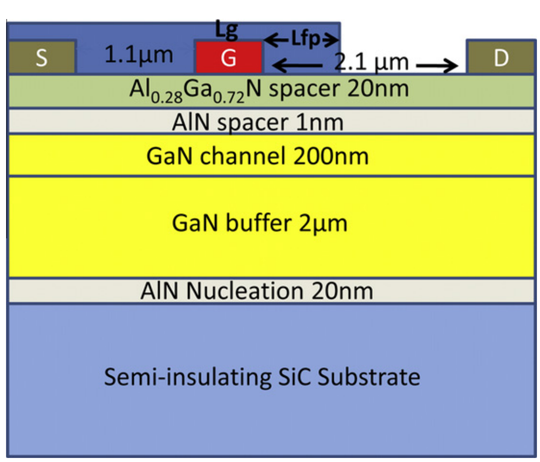

Fig. 1. Cross-section of the fabricated devices. The gate to drain distance L_{gd} = 2.1 μm, gate width W_g = 80 μm, gate length L_g = 0.8 μm, 2 μm and 3 μm were fabricated.

3. Results and discussion

The fabricated devices first underwent a reverse-biased stress test. Shown in Fig. 2 is a plot of the drain to source leakage current (I_{ds}) versus drain voltage (V_{ds}) as a function of temperature at the pinch-off voltage of V_{gs} = −5 V. In order to degrade the devices in a controllable manner, the drain voltage was biased from 0 V to 20 V to investigate the drain to source leakage current from room temperature to 425 K. A substantial reduction of the drain to source leakage was obtained. I_{ds} decreased from 7.3×10^{-3} A/mm at room temperature (*RT*) to 5.8×10^{-3} A/mm at *T* = 375 K. This is quite similar to what was reported by Ohno et al. [10]. They concluded that the breakdown voltage had a positive temperature coefficient because of the impact ionization-dominated breakdown in the channel.

However, in our experiment, I_{ds} was found to be increased with further increase in temperature to over *T* = 375 K. In order to investigate the reason for the observed V_{ds}–I_{ds}–T characteristics, the DUT was cooled down from 425 K to *RT* and the I_{ds} leakage current versus V_{ds} was re-measured as a function of *T*. The results are as shown in Fig. 3. The leakage current increases as a function of *T*, while the measured breakdown voltage at I_{ds} = 0.025 A/mm has a negative temperature coefficient of approximately −0.113 V/K. To verify the phenomenon that the increase of the I_{ds} and the reduction of the breakdown voltage are permanent, one sample was allowed to cool down and the other sample received thermal

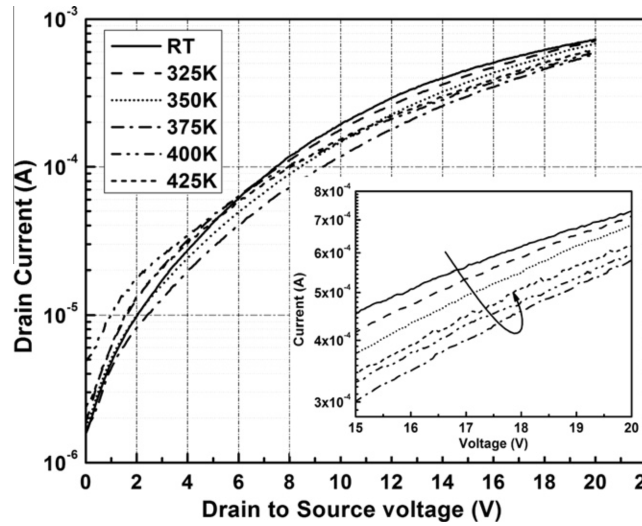

Fig. 2. Measured I_{ds}–V_{ds}–T characteristics of drain leakage current. The gate to drain distance L_{gd} = 2.1 μm, gate width W_g = 80 μm, V_g = −5 V.

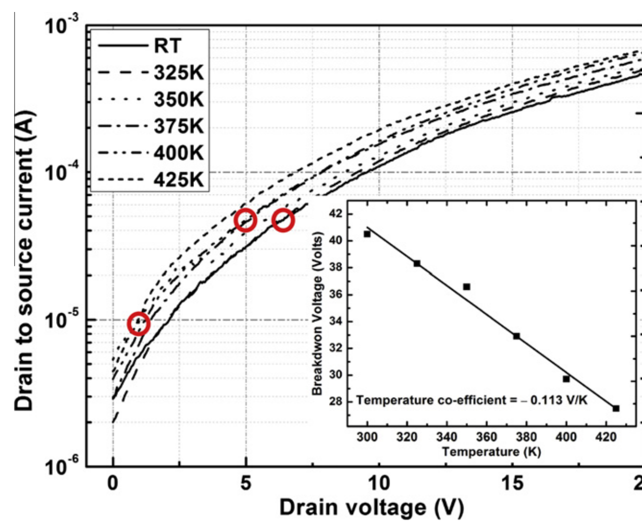

Fig. 3. I_{ds}–V_{ds}–T characteristics of drain leakage current after thermal annealing. The gate to drain distance L_{gd} = 2.1 μm, gate width W_g = 80 μm, V_g = −5 V.

annealing stress at *T* = 425 K. Both devices were treated overnight (for more than 12 h). The third sample only received a thermal annealing of 425 K for 5 min and allowed to cool down at room temperature. No noticeable changes among the samples were found in V_{ds}–I_{ds}–T characteristics as shown in Fig. 3. A possible explanation is that the surface mobile charges are the main reason which attributed to the positive breakdown coefficient observed in Fig. 2. As temperature increased from *RT* to 325 K as shown in Fig. 3, the leakage current for the *RT* sample was also increased at low voltage operation (<5 V). However, the leakage current was found to have decreased for voltage range of over 5 V when compared to the device held at 325 K, due to the increased Schottky barrier height. Other temperature dependent mechanisms, which will be discussed below when the device operated under higher temperatures (>325 K), are more severe than just an increase in barrier height. The intersection moved towards the left side (red[1] circles). With regard to the negative breakdown temperature coefficient, the diodes [12] based on similar structure also

[1] For interpretation of color in Fig. 3, the reader is referred to the web version of this article.

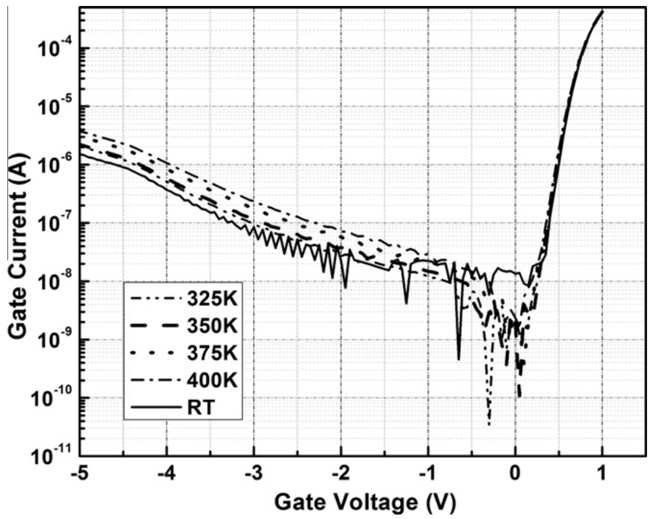

Fig. 4. Typical I_g–V_g–T curves of Ni/Au Schottky contacts with gate length of 0.8 μm, width of 80 μm on AlGaN/GaN heterstructures. Gate current is the absolute value.

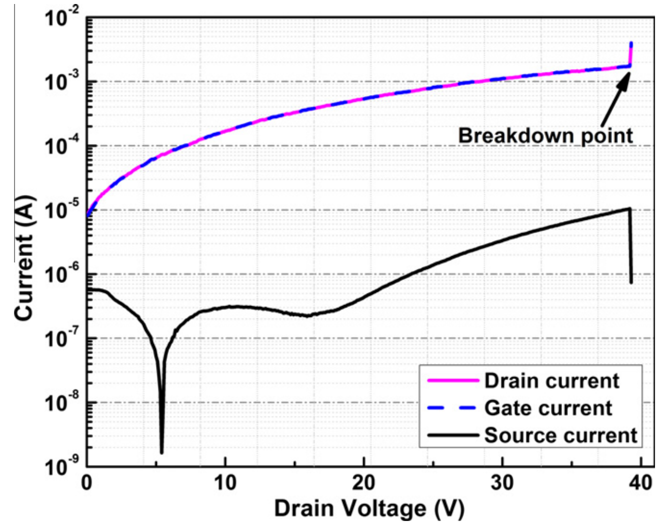

Fig. 5. I_d, I_g, I_s curves after the sample biased to breakdown, I_d, I_g and I_s are the absolute value, T = 300 K.

showed a negative temperature coefficient. The switch to positive coefficient was only seen as the defect density in the material was improved. The power AlGaN/GaN HEMTs fabricated based on a *RF* process were well passivated using a Si_3N_4 film. This suggests that the dominant mechanism for breakdown is trap/defect-related rather than surface hopping conduction.

The origin of the gate leakage current was also investigated. In order to study the gate leakage current in the power AlGaN/GaN HMET, I_g versus V_g characteristics were measured at different temperatures. Fig. 4 shows I_g as a function of V_g. The drain electrode was shorted to the source ($V_d = V_s = 0$ V). V_g was swept from −5 V to 1 V.

From Fig. 4, the gate leakage current was measured to be 1.49×10^{-6} A at room temperature and 3.7×10^{-6} A at $T = 400$ K. Since the thermionic emission current is strongly dependant on the temperature as suggested by the equation below:

$$J \propto -AT^2 \exp(-q\varphi_{bn}/KT) \quad (1)$$

where A is the effective Richardson constant; T is the absolute temperature; q is the electron charge; K is the Boltzmann's constant; φ_{bn} is the Schottky barrier height. The observed temperature independent behavior suggests that the gate leakage current in the fabricated AlGaN/GaN HEMTs is not dominated by thermionic emission but by trap/defect tunneling. This tunneling current is more sensitive to temperatures than the Schottky barrier heights, which explains the intersection of the I–V curves as shown in Fig. 3. The surface process can improve AlGaN Schottky interface properties as a result of reduction in the amount of VN-related (Nitrogen Vacancy) defects and oxygen impurities [13]. Further study is necessary to clarify this point.

In order to further investigate the breakdown failure mechanism of the AlGaN/GaN HEMTs, the device was biased to near breakdown condition. Currents that flow through the three electrodes were monitored and are as illustrated in Fig. 5.

The drain and gate leakage currents increase simultaneously and show exactly the same value. "Soft" breakdown was observed over most of the voltage range. "Hard" breakdown occurs when the leakage current reaches a certain critical value (2×10^{-3} A in this case). The abrupt increase of the gate to drain leakage suggests that an irreversible electron current pathway was developed from the gate directly to the 2-DEG region after onset of device degradation. This relatively high current flowing through the gate metal may have caused the thermal damage of the device as shown in Fig. 6.

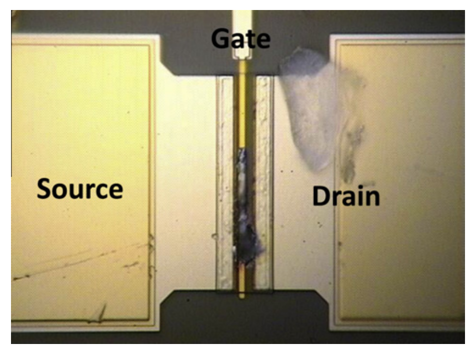

Fig. 6. Image of a representative breakdown failure sample without field plate.

The breakdown voltage and gate leakage current as a function of gate length were plotted in Fig. 7. The breakdown voltage is increased from around 36 V to 41.5 V while the leakage current is decreased from 1.68×10^{-5} A/mm to 1.47×10^{-5} A/mm, indicating that the effect of trap/defect-assisted intrinsic Schottky tunneling was reduced due to the reduction of the Schottky gate area. Device requires higher electric field induced injection to form the current pathway. Thus breakdown can be improved to some extent.

Devices with source field plate were also fabricated. The measured breakdown voltage and temperature coefficient as a function of source field plate (L_{fp}) are as shown in Fig. 8. From Fig. 9, the breakdown increased from 40 V to 138 V when a field plate length of 1.6 μm was used. The temperature coefficient of the breakdown voltage changed from −0.113 V/K for the conventional HEMT without field plate to −0.065 V/K with a field plate length of 1.6 μm. Leakage-dominated breakdown was less pronounced due to suppression of the hot carrier injection.

In addition, breakdown occurred with substantially lower leakage current (I_{ds}) with $L_{fp} > 0.4$ μm (see Fig. 8), indicating that premature breakdown may have occurred near the edge of the field plate as shown in Fig. 10.

There are two factors which may govern the breakdown mechanisms for devices with field plate structures: gate electrode tunneling leakage at the drain side gate edge due to hot electrons, and electric field induced surface breakdown at the edge of the field plate. The lower leakage current I_{ds} with $L_{fp} > 0.4$ μm, as shown in Fig. 8, indicates that the electric field near the gate edge was effectively suppressed. Breakdown was dependant on the low-

Please cite this article in press as: Xie G et al. Study of the breakdown failure mechanisms for power AlGaN/GaN HEMTs implemented using a *RF* compatible process. Microelectron Reliab (2011), doi:10.1016/j.microrel.2011.11.022

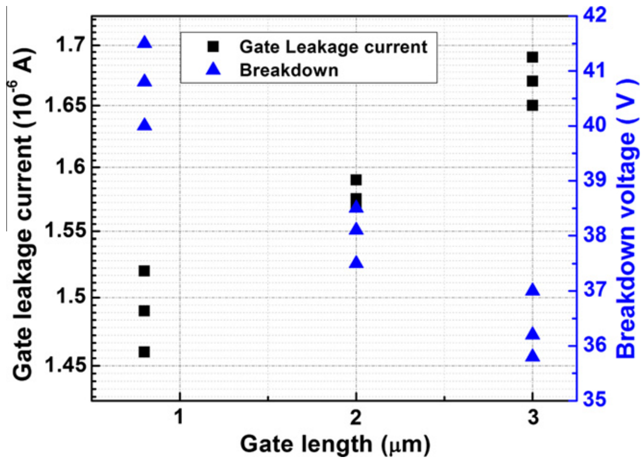

Fig. 7. Plotted breakdown voltage and gate leakage current as a function of gate length. I_g @ $V_d = V_s = GND$, $V_g = -5$ V, $W_g = 80$ μm, $T = 300$ K.

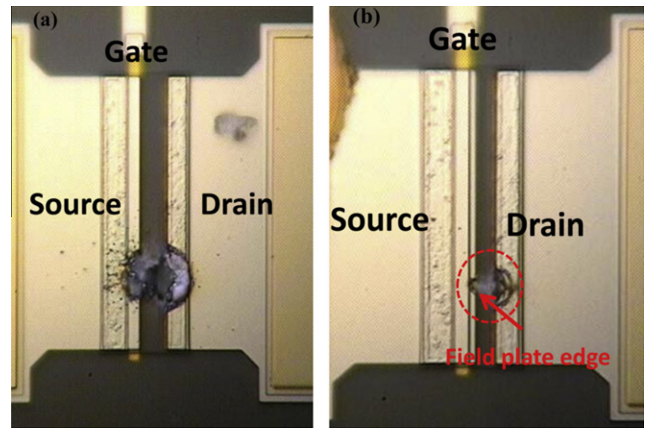

Fig. 10. Image of a representative of breakdown failure sample. (a) $L_{fp} = 0.2$ μm (b) $L_{fp} = 0.4$ μm, $T = 300$ K.

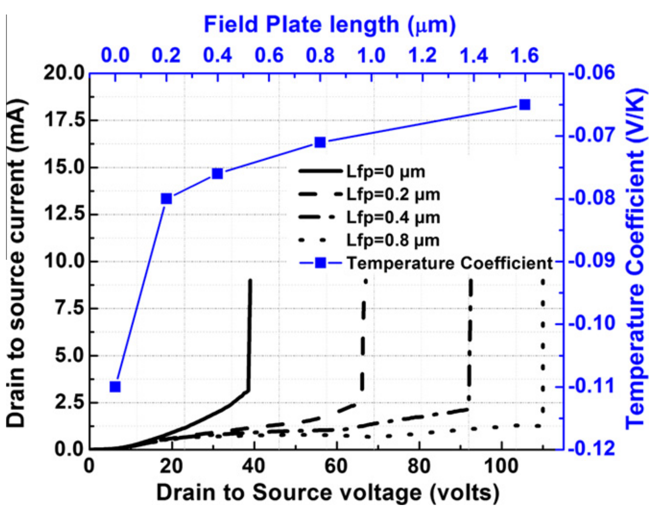

Fig. 8. Measured breakdown voltage and temperature coefficient as a function of source field plate (L_{fp}). $V_g = -5$ V, $L_g = 0.8$ μm, $W_g = 80$ μm.

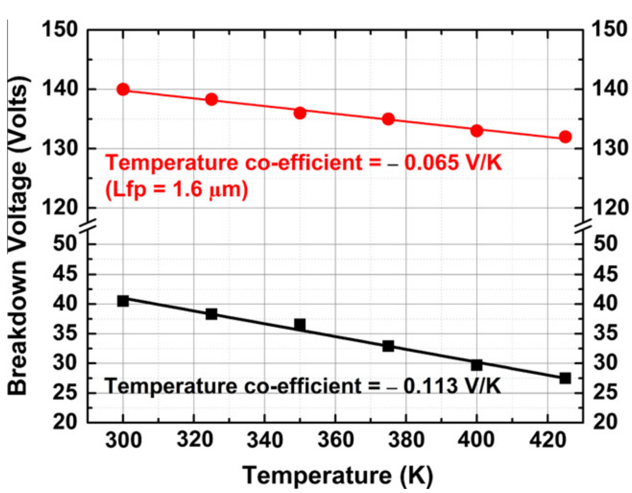

Fig. 9. Breakdown voltages as a function of temperature for conventional HEMT without field plate and with field plate of $L_{fp} = 1.6$ μm.

er threshold of the gate leakage and electric field strength near the field plate edge. Meanwhile, the negative temperature coefficient for the breakdown voltage with field plate structures indicate that the breakdown is still dominated by trap/defect assisted gate tunneling rather than impact ionization in the channel.

4. Conclusions

In summary, the breakdown degradation under high temperature operation and breakdown failure mechanism for power AlGaN/GaN HEMTs fabricated using a *RF* process were investigated. Temperature dependent measurement for devices with and without field plate showed that there are two components for the leakage current which can both attribute to the device breakdown failure: electric field near the drain side gate edge induced injection from the gate metal to the channel and the initial/generated trap/defect-assisted gate tunneling leakage. The irreversible current pathway developed causes an abrupt increase in the drain to gate current. Temperature coefficient of the breakdown was lowered when field plate was applied. Electron injection was suppressed while breakdown voltage was still limited by lower threshold of the gate tunneling and electric field strength near the field plate edge. These results indicate that the gate length should be minimized based on the *RF* process to decrease the leakage and increase the operational frequency for the sub 200 V power HEMT applications with less negative temperature coefficient of breakdown by using field plate. Thickness of the passivation film should also be optimized to relieve the electric field concentration near the field plate and prevent premature breakdown.

Acknowledgments

The authors would like to gratefully acknowledge the financial support from the China Scholarship Council (*File No.* 2009607040), Auto 21, a Network of Centers of Excellence in Canada. Special thanks go to Canadian Microelectronics Corporation, Canada for providing valuable technical support and fabrication.

References

[1] Chow TP, Tyagi R. Wide bandgap compound semiconductors for superior high-voltage unipolar power devices. IEEE Trans. Electron. Dev. 1994;41(8):1481–3.
[2] Yoder MN. Wide bandgap semiconductor materials and devices. IEEE Trans. Electron. Dev. 1996;43(10).
[3] Hudgins JL, Simin GS, Santi E, Khan MA. An assessment of wide bandgap semiconductors for power devices. IEEE Trans. Power Electron. 2003;18(3).

Please cite this article in press as: Xie G et al. Study of the breakdown failure mechanisms for power AlGaN/GaN HEMTs implemented using a *RF* compatible process. Microelectron Reliab (2011), doi:10.1016/j.microrel.2011.11.022

[4] Wang Xiaoliang, Wang Zhangguo. AlGaN/AlN/GaN/SiC HEMT structure with high mobility GaN thin layer as channel grown by MOCVD. J. Cryst. Growth 2007;298:835–9.
[5] Mizuno Shinya, Ohno Yutaka, Kishimoto Shigeru, Maezawa Koichi, Mizutani Takashi. Large gate leakage current in AlGaN/GaN high electron mobility transistors. Jpn. J. Appl. Phys. 2002;41:5125–6.
[6] U.K. Mishra, N.Q. Zhang, Status of AlGaN/GaN HEMTs for microwave and power switching applications, Int. Symp. Compound Semiconductors, Tokyo, Japan, 2001.
[7] Bahat-Treidel Eldad, Hilt Oliver, Brunner Frank, Sidorov Victor, Würfl Joachim, Tränkle Günther. AlGaN/GaN/AlGaN DH-HEMTs breakdown voltage enhancement using multiple grating field plates (MGFPs). IEEE Trans. Electron. Dev. 2010;57(6).
[8] A. Hidekazu Umeda, Y. Suzuki, Anda, M. Ishida, T. Ueda, T. Tanaka, D. Ueda, Blocking-voltage boosting technology for GaN transistors by widening depletion layer in Si substrates, IEEE Electron Devices Meeting, San Francisco, CA, 2010.
[9] Arulkumaran S, Egawa T, Ishikawa H, Jimbo T. Temperature dependence of gate-leakage current in AlGaN/GaN high-electron-mobility transistors. Appl. Phys. Lett. 2003;82:3110.
[10] Ohno Yutaka, Nakao Takeshi, Kishimoto Shigeru, Maezawa Koichi, Mizutani Takashi. Effects of surface passivation on breakdown of AlGaN/GaN high-electron-mobility transistors. Appl. Phys. Lett. 2002;84(12).
[11] Kotani Junji, Tajima Masafumi, Kasai Seiya, Hashizume Tamotsu. Mechanism of surface conduction in the vicinity of Schottky gates on AlGaN/GaN heterostructures. Appl. Phys. Lett. 2007;91:093501.
[12] Voss Lars, Gila BP, Pearton Sj, Wang Hung-Ta, Ren F. Characterization of bulk GaN rectifiers for hydrogen gas sensing. J. Vac. Sci. Technol. B 2005;23:2373.
[13] Hashizume Tamotsu, Kotani Junji, Basile Alberto, Kaneko Masamitsu. Surface control process of AlGaN for suppression of gate leakage currents in AlGaN/GaN heterostructure field effect transistors. Jpn. J. Appl. Phys. 2006;45:L111–3.

Please cite this article in press as: Xie G et al. Study of the breakdown failure mechanisms for power AlGaN/GaN HEMTs implemented using a *RF* compatible process. Microelectron Reliab (2011), doi:10.1016/j.microrel.2011.11.022